Title	Optical reflectivity of spin-coated multilayered ZnO and Al:ZnO Thin Films
Author(s)	Buckley, Darragh; McCormack, Robert; McNulty, David; Zubialevich, Vitaly Z.; Parbrook, Peter J.; O'Dwyer, Colm
Publication date	2017-05
Original citation	Buckley, D., McCormack, R., McNulty, D., Zubialevich, V. Z., Parbrook, P. J. and O'Dwyer, C. (2017) 'Optical Reflectivity of Spin-Coated Multilayered ZnO and Al:ZnO Thin Films', ECS Transactions, 77(6), pp. 75-82. doi: 10.1149/07706.0075ecst
Type of publication	Article (peer-reviewed)
Link to publisher's version	http://ecst.ecsdl.org/content/77/6/75.abstract http://dx.doi.org/10.1149/07706.0075ecst Access to the full text of the published version may require a subscription.
Rights	**© 2017 ECS - The Electrochemical Society**
Item downloaded from	http://hdl.handle.net/10468/6174

Optical Reflectivity of Spin-Coated Multilayered ZnO and Al:ZnO Thin Films

Darragh Buckley[1], Robert McCormack[1], David McNulty[1], Vitaly Zubialevich[2], Peter Parbrook[2,3], and Colm O'Dwyer[1,2]

[1] Department of Chemistry, University College Cork, Cork T12 YN60, Ireland
[2] Tyndall National Institute, Lee Maltings, Cork T12 R5CP, Ireland
[3] Department of Electrical & Electronic Engineering, University College Cork, Cork T12 YN60, Ireland

Abstract

Controlling growth, doping, crystallization, thickness of thin films of thin film transistor (TFT) channel materials is required in order to improve and control physical properties, primarily electronic conductivity and optical transparency. With the advent of flexible electronics and curved TFT-based display panels, low cost, solution-processed methods are important and provide scalable coating methods on a range of substrates. This work demonstrates the changes to the morphology, crystalline structure, optical reflectivity and electrical conductance of solution-processed ZnO thin films by the inclusion of an aluminium dopant during spin-coating. The measurements also determine the compositional chemical state of the Al:ZnO structures compared to ZnO using X-ray photoelectron spectroscopy in conjunction with detailed X-ray diffraction and transmission electron microscopy examination of the film morphology.

Introduction

Zinc oxide (ZnO) and its doped counterparts such as Al:ZnO are extensively investigated as indium-free alternatives for oxide electronics including solar cells, light emitting diodes and also display technologies. For the latter application, thin film transistor (TFT) devices are the building-block structures.(1) High fidelity TFTs require conductive channel materials, with good field effect mobility for majority carriers and tunable optical transparency. Controlling growth, doping, crystallization, thickness of thin films of thin film transistor (TFT) channel materials is required in order to improve and control physical properties, primarily electronic conductivity and optical transparency. With the advent of flexible electronics and curved TFT-based display panels, low cost, solution-processed methods are important and provide scalable coating methods on a range of substrates.

Transparent conductive oxides (TCOs) have attracted much interest in the area of optoelectronics due to their ability to have controllable conductivity and carrier mobility, while maintaining high optical transparency.(2-7) Zinc oxide (ZnO) and its doped counterparts such as Al:ZnO (AZO) are researched for use in many key optoelectronic devices such as TFTs(8), photovoltaics(9), solar cells(10) and electrochromics(7). In particular, zinc oxide (ZnO) attracted the initial attention in this area due to its wide, direct band gap ($E_g \sim 3.3$ eV at 300 K)(11) and a crystal lattice allows for interstitial doping.(12)

Despite these benefits, ZnO does not meet the electrical performance of other doped metal oxides, such as Sn-doped In_2O_3 (ITO), owing to a lower majority carrier

concentration.[13, 14] ITO is currently one of the most popular semiconducting material used in the area of optoelectronics particularly in flat-panel displays due to its wide band gap (>3 eV).[15] However, there is a drive to replace ITO with ZnO its doped forms such as In-doped ZnO (IZO), In-Ga-Zn-O (IGZO) and Al-doped ZnO.[1] For AZO, the composition serves as an indium-free alternative which lowers expense due to the higher relative abundance in the Earth's crust (75 ppm for Zn opposed to 0.16 ppm for In).[13]

Altering the carrier concentration of a metal oxide such as ZnO with the addition of an interstitial dopant will also affect the optical properties.[16] The refractive index of the material, dielectric constant and plasma frequency are all modulated by the charge carrier concentration while the band-gap can also be widened by the stresses produced in the crystal lattice from the inclusion of a dopant atom.[17-19] Optical reflectivity, which is subject to change with the addition of a dopant, is of key importance to materials researched in optoelectronics, particularly in transparent TFT devices and solar cells. [20, 21] Controlling growth, doping, crystallization, thickness of thin films of these materials is required in order to improve and control physical properties, primarily electronic conductivity and optical transparency. With the advent of flexible electronics and curved TFT-based display panels, low cost, solution-processed methods are important and provide scalable coating methods on a range of substrates.

In this work, multilayered or homogeneous quasi-superlattices of metal oxides with a single composition for TFTs are displayed as dispersive materials that behave as continuous thin films with thickness controlled by cumulative spin-coating. We show that crystalline, epitaxial-like thin films can be deposited from a liquid in open atmosphere via spin-coating and that the formation of a quasi-superlattice (QSL) structure through an iterative deposition method is possible. Analysis of these films in order to determine crystallinity and internal structure is determined through X-ray diffraction and transmission electron microscopy (TEM). Angle-resolved reflectance for a single-layer and multilayer samples grown on oxidized silicon substrates are acquired to define the growth conditions and processing to provide tuneable antireflection coatings of ZnO and AZO.

Experimental

ZnO thin films were prepared from a 0.75M solution of zinc acetate dihydrate [$Zn(CH_3COO)_2.2H_2O$] dissolved in 2-methoxyethanol [$CH_3OCH_2CH_2OH$]. A solution of monoethanolamine was added to this zinc acetate solution to act as a stabilising agent in a molar ratio of 1:1. In order to prepare Al:ZnO (AZO) films of ~5 mol% Al, an Al-solution was prepared by dissolving 0.1407 g of aluminium nitrate-nonahydrate [$Al(NO_3)_3.9H_2O$] in 10 mL of 2-methoxyethanol. This solution was added to the 0.75 M zinc acetate solution and stirred for 2 hours at 60 °C.

All thin films samples were deposited onto silicon wafers covered with 85 nm of thermally grown SiO_2, cleaved to 2 cm × 2 cm in size. Prior to deposition, substrates were cleaned via sonication in acetone, IPA and DI water and then received a 30 min UV-ozone treatment using a Novascan UV ozone system. Films were deposited from liquid precursors using a SCS G3 desktop spin coater. Substrates were coated and spun at 3,000 rpm for 30 s, including a 5 s ramp time. Following this, samples were dried for 5 min between 250 - 270 °C in an open-air convection oven. This deposition process can be repeated as many times as desired to create the quasi-superlattice (QSL) structure before samples undergo a final annealing treatment at 300 °C for 1 hr.

Transmission electron microscopy (TEM) was conducted on cross-sectioned lamellae of ZnO and AZO thin films. TEM analysis was conducted using a JEOL JEM-2100 TEM operating at 200 kV. Lamella from samples were prepared for TEM analysis by cross-sectioning using an FEI Helios Nanolab Dual Beam Focused-ion Beam (FIB) System. X-ray diffraction (XRD) was used to characterise the crystallographic structure of the single and multi-layer ZnO and AZO films after spin coating deposition using a Philips X'Pert PW3719 diffractometer using Cu Kα radiation (40 kV and 35 mA) scanned between 10 - 80° (2θ).

Angle-resolved optical characterisation was conducted using an in-house constructed cage-mounted optical reflectance/transmission spectroscopy setup. Samples were illuminated with a white tungsten halogen lamp (output spectral range from 360 - 2,400 nm) collimated to a beam diameter of ~ 1 - 2 mm using optical fiber. The reflected light was collected using focusing optics into an Oceanoptics USB2000+ spectrometer (400 – 1,000 nm range) which has an optical resolution of 1.5 nm. The reflected light was also collected in the same manner using an Oceanoptics NIRQuest 512-2.5 to obtain the NIR reflectance spectra (1,000 – 2,500 nm range) which has an optical resolution of 6.3 nm. Reference spectra were acquired using an Au mirror (ThorLabs gold mirror PF10-03-M01) at each angle of incidence investigated. To examine the anti-reflection properties of ZnO and AZO thin films at various wavelengths and angles of incidence, spectroscopic measurements were taken at four angles of incidence, $\theta_i =$ 30°, 60°, 45° and 75°.

Results and discussion

ZnO and AZO thin films, prepared on Si/SiO$_2$ substrates, were examined via TEM on FIB-thinned lamella. This was conducted to determine the internal structure resulting from the iterative process of spin-coating with a drying step before final annealing. TEM images of 20 layer ZnO and AZO QSLs are shown in Figure 1. The thickness of these films is very uniform throughout and the number of deposited layers can be seen from the cross-section of the layered internal structure. Due to the method of deposition, the films do form a multilayered QSL structure, in place of a continuous bulk of crystalline ZnO or AZO. Inset in Figure 2(b) shows the clear bilayer structure of each of the deposited layers. The bulk of the deposited material forms a more porous mid-layer while a dense capping layer forms as a result of the short drying step between each deposition (5 min at 260 °C). Films are subsequently crystallized by a 300 °C annealing for one hour.
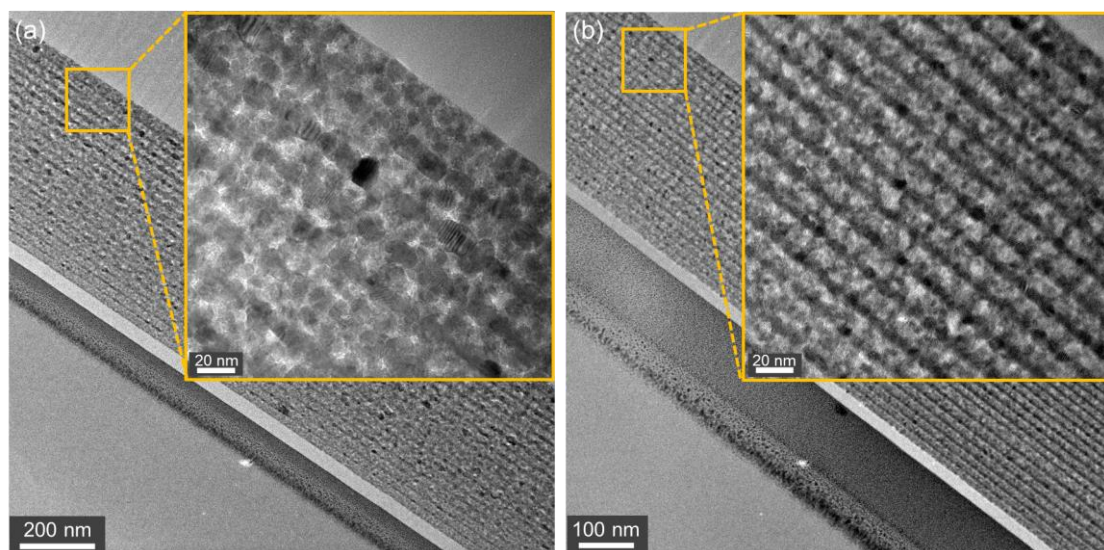

Figure 1. TEM cross-sectional images of (a) 20 layer ZnO and (b) 20 layer AZO thin films.

QSLs produced from liquid spin coating on amorphous substrates produce highly crystalline thin films in most cases. Figure 2 displays the X-ray diffraction patterns for 1 and 20 layer ZnO and AZO thin films. The ZnO samples display very high crystal quality, with a clear change in growth orientation with the increased number of depositions. The single layer ZnO sample shows a reflection in the $[10\bar{1}0]$ m-plane only with no other [*hkil*] reflections present. Similarly, the 20 layer QSL of ZnO shows the same m-plane growth but also a dominant reflection in the [0002] direction, which corresponds to the c-plane. As a result of the formation of dense capping layers with iterative depositions, the crystal growth orientation changes from the m-plane to the c-plane. For the AZO QSL, a minor reflection in the [0002] direction can be seen, indicating crystal growth in the c-plane direction, similar to the ZnO QSL. The single layer AZO film however appears amorphous, a possible result of the Al addition to the ZnO lattice causing a necessary increase in the heat energy required to crystallise the film. Further work is required to investigate the heat energy requirements for the fabrication of single-layer AZO thin films.
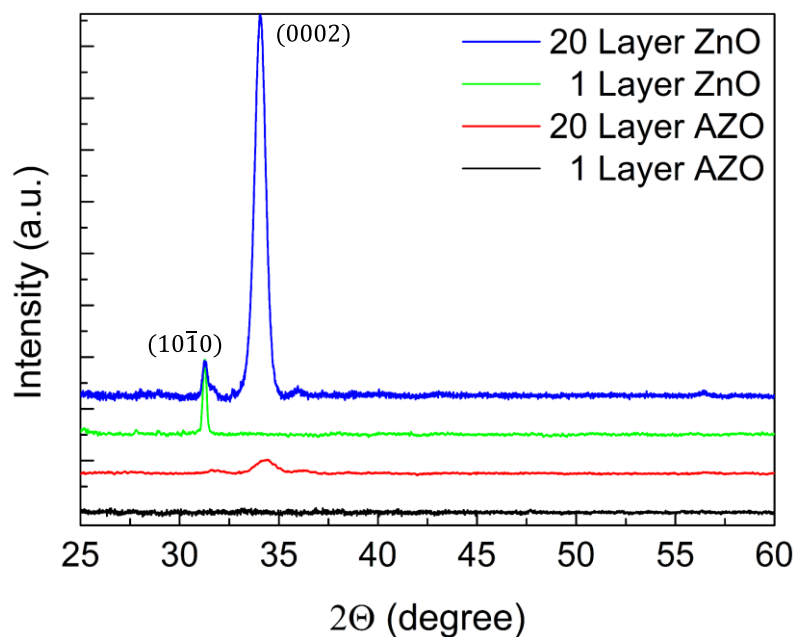

Figure 2. X-ray diffraction patterns for 1 and 20 layer ZnO and AZO thin films.

Figure 3 shows the reflectance spectra for 1 and 20 layer ZnO and AZO in the UV-vis-NIR range (400 nm – 2500 nm). The single layer thin films for both materials display a low average reflectance across the UV-vis-NIR range, which corresponds to a high transparency, similar to IZO. This is shown to increase with the number of iterative depositions. For multilayer QSLs the reflectance increases at certain wavelengths to >40%. Reflectance data shows that the 20 layer QSL films behave optically as coherent thin films. The reflectance spectra for the 20 layer QSL films show that the material is dispersive at longer wavelengths, with peaks at lower energy wavelengths exhibiting lower reflectance intensities. The broadband reflectance spectra for ZnO and AZO are similar as expected for single and multilayered systems. The addition of a dopant to the ZnO lattice can alter defect absorption and induce lattice stresses. As a result, spectra are blue-shifted by ~40 nm for AZO compared to ZnO.

We have previously shown[14] that determination of the optical thickness of these ZnO and AZO films is possible from the broadband reflectance spectra using an adapted method from thin film optical interference, and that thinner films have a better agreement with predicted optical thickness measured via TEM.

At energies below the bandgap in semiconducting metal oxides, Urbach states, defect absorption, processes involving multiphonon interactions and scattering can all increase reflectivity. Urbach and defect absorption is likely in our films, since the sub-band photoluminescence shows several emission features, and TEM data in Fig. 1 confirms granular features in part of the periodic structure in films that exhibit a high degree of crystalline orientation as a layer.
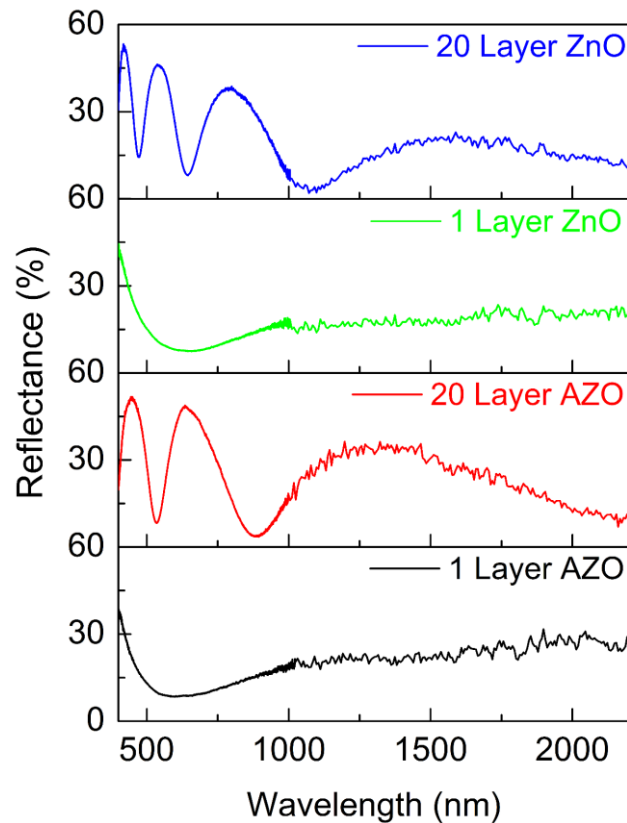

Figure 3. UV-vis-NIR reflectance spectra of single- and multi-layer ZnO and AZO thin films acquired at angle of incidence, $\theta_i = 45°$.

The effect on varying the angle of incidence on the resulting reflectance spectra is shown in Fig. 4. Similar to Fig. 3 which displays the spectra collected at $\theta_i = 45°$, the spectra exhibit characteristic wavelength dependent interference from half-wave and quarter-wave optical thickness (QWOT) variation. As can be seen from Fig. 4, we observed an increase in the average reflectance for all films (1 and 20 layer, ZnO and AZO) at an incident angle of 75°. Characterizing angles where the anti-reflections are optimal is crucial for materials integrated in optoelectronic devices and solar cells. As with the spectra taken at $\theta_i = 45°$ from Fig. 3, the AZO reflectance spectra are blue-shifted in relation to the ZnO spectra by ~ 40 nm. The spectra display characteristic interference based on incident light wavelength between ZnO and AZO, however for the ZnO QSL measured at $\theta_i = 75°$ we observe a unique response based on interference that exhibits behavior different to that measured at 60° and 30°. As thicker films of ~20 layers approach a thickness value roughly equal to the wavelength of the incident light, the effects of destructive and constructive interference are expected to be more pronounced on the resulting reflectance spectra.
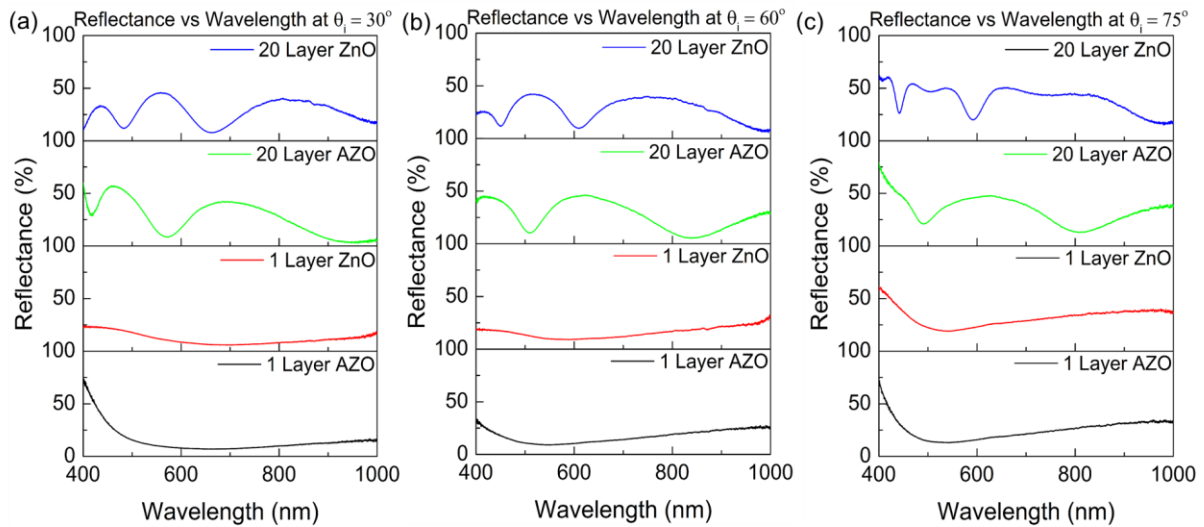
Figure 4. Angle dependent reflectance spectra of ZnO and AZO thin films acquired at various angles of incidence, θ_i = (a) 30°, (b) 60° and (c) 75°.

The wavelength at which the minimum percentage reflectance for single layer ZnO was found to be at λ = 657 nm. The reflectance of the ZnO 20 layer QSL was then examined at this wavelength to characterize the evolution of the films reflectance as a function of number of depositions and QSL film thickness. This process was repeated for all of the measured angles of incidence (θ_i = 30°, 45°, 60° and 75°). The same analysis was applied to the AZO samples where the minima for 1 layer AZO was found to be 599 nm. The resultant polar plots are shown in Fig. 5. For the QSLs of both materials, we note a definite increase in the reflectance at higher angles compared to single layer films, with values for ZnO and AZO both reaching >40% total reflectance at 75°. The single layer AZO films show a much less reflective behaviour than the pure ZnO counterparts when examine at multiple angles, showing consistently <20% reflectance when measured at the selected minima. This shows a reliable anti-reflection use for very thin AZO films for light ~ 600 nm. Figure 5 highlights that both sets of films maintain a consistently low (<30%) reflectance when examined at 45° or lower angles. At higher angles, QSL films appear to be ~3 times more reflective.
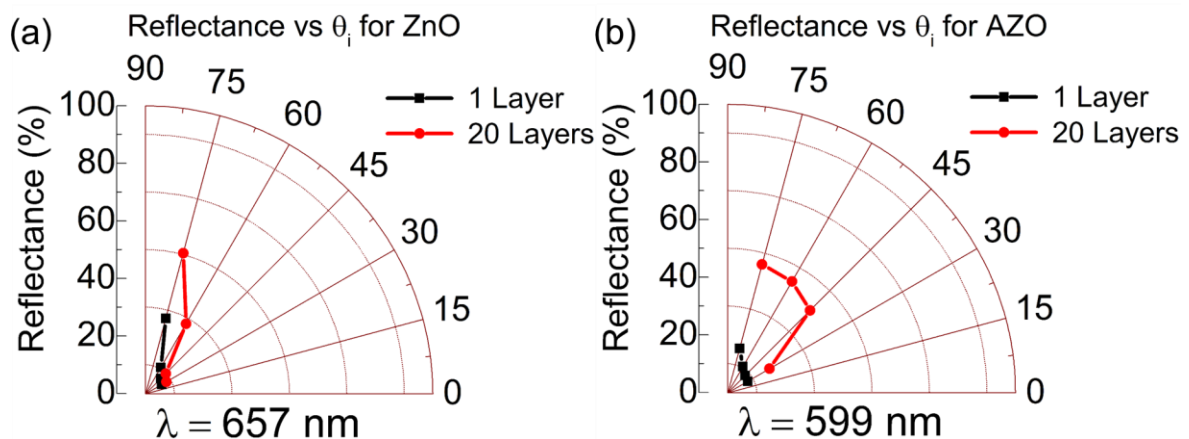

Figure 5. Reflectance measurements of 1 and 20 layer ZnO and AZO thin films at wavelengths corresponding to reflectance minima from single layer ZnO and AZO respectively.

Conclusions

The growth of crystalline thin films in an epitaxial-like quasi-superlattice is demonstrated. Films with periodic structures which are clearly visible via microscopy are deposited from a solution-based process on amorphous substrates. Highly crystalline and ordered ZnO films display a change in crystalline texture from the m-plane for 1 layer films to predominantly c-axis orientation upon further deposition of material. With the addition of an Al dopant, films show a more amorphous texture, with a 20 layer QSL still displaying c-plane growth preference, indicating that a higher processing temperature may be required for production of highly crystalline AZO. Films studied using broadband reflectance spectroscopy show dispersive behavior at longer wavelengths with periodic minima and maxima shown based on wavelength dependent interference effects. We have shown the behaviour of single layer samples and multilayer QSLs under a variety of different angles of incidence to characterise the anti-reflection properties of ZnO with and without an Al dopant. AZO single layer films anti-reflective compared to ZnO, particularly at low angles, yet QSLs for both materials show a substantial increase in reflectance at high angles of incidence.

Acknowledgements

References

1. X. Yu, T. J. Marks and A. Facchetti, *Nat. Mater.*, **15**, 383 (2016).
2. E. Fortunato, P. Barquinha, A. Pimentel, A. Gonçalves, A. Marques, L. Pereira and R. Martins, *Thin Solid Films*, **487**, 205 (2005).
3. C. Glynn and C. O'Dwyer, *Adv. Mater. Interfaces*, **4**, 1600610 (2017).
4. C. Glynn, H. Geaney, D. McNulty, J. O'Connell, J. D. Holmes and C. O'Dwyer, *J. Vac. Sci. Technol. A*, **35**, 020602 (2017).
5. C. Glynn, D. Aureau, G. Collins, S. O'Hanlon, A. Etcheberry and C. O'Dwyer, *Nanoscale*, **7**, 20227 (2015).
6. R. M. Pasquarelli, D. S. Ginley and R. O'Hayre, *Chem. Soc. Rev.*, **40**, 5406 (2011).
7. C. G. Granqvist, *Thin Solid Films*, **564**, 1 (2014).
8. K. K. Banger, Y. Yamashita, K. Mori, R. L. Peterson, T. Leedham, J. Rickard and H. Sirringhaus, *Nat. Mater.*, **10**, 45 (2011).
9. C. P. Chen, Y. D. Chen and S. C. Chuang, *Adv. Mater.*, **23**, 3859 (2011).
10. T. P. Chou, Q. Zhang, G. E. Fryxell and G. Z. Cao, *Adv. Mater.*, **19**, 2588 (2007).
11. Ü. Özgür, Y. I. Alivov, C. Liu, A. Teke, M. A. Reshchikov, S. Doğan, V. Avrutin, S.-J. Cho and H. Morkoç, *J. Appl. Phys.*, **98**, 041301 (2005).
12. D. C. Look, in *Zinc Oxide Bulk, Thin Films and Nanostructures*, p. 21, Elsevier Science Ltd, Oxford (2006).
13. A. Lyubchyk, A. Vicente, B. Soule, P. U. Alves, T. Mateus, M. J. Mendes, H. Águas, E. Fortunato and R. Martins, *Adv. Electron. Mater.*, **2**, 1500287 (2016).
14. E. Fortunato, A. Gonçalves, A. Pimentel, P. Barquinha, G. Gonçalves, L. Pereira, I. Ferreira and R. Martins, *Appl. Phys. A.*, **96**, 197 (2009).

15.   A. Lyubchyk, A. Vicente, P. U. Alves, B. Catela, B. Soule, T. Mateus, M. J. Mendes, H. Águas, E. Fortunato and R. Martins, *Phys. Status Solidi A*, **213**, 2317 (2016).
16.   X. D. Li, T. P. Chen, Y. Liu and K. C. Leong, *Opt. Express*, **22**, 23086 (2014).
17.   B. E. Sernelius, K. F. Berggren, Z. C. Jin, I. Hamberg and C. G. Granqvist, *Phys. Rev. B.*, **37**, 10244 (1988).
18.   P. D. C. King and T. D. Veal, *J. Phys. Condens. Matter.*, **23**, 334214 (2011).
19.   H. K. Raut, V. A. Ganesh, A. S. Nair and S. Ramakrishna, *Energ. Environ. Sci.*, **4**, 3779 (2011).
20.   D. Buckley, R. McCormack and C. O'Dwyer, *J. Phys. D: Appl. Phys.* doi: 10.1088/1361-6463/aa6559 (2017).
21.   C. O'Dwyer, M. Szachowicz, G. Visimberga, V. Lavayen, S. B. Newcomb and C. M. S. Torres, *Nature Nanotech.*, **4**, 239 (2009).